

Dark Matter Cosmology with Varying Viscosity: a Possible Resolution to the S_8 Tension

Amjad Ashoorioon and Zahra Davari

School of Physics, Institute for Research in Fundamental Sciences (IPM), P.O. Box 19395-5531, Tehran, Iran

April 17, 2023

ABSTRACT

We study varying forms of viscous dark matter and try to address the intriguing tensions of the standard model of cosmology with the recent cosmological data, including the Hubble and S_8 tensions. We note that assuming the dark matter viscosity depends on the Hubble parameter, dark matter density, or both, one can improve the statistics. Although the models tend to aggravate the Hubble tension a bit, they tend to reduce the S_8 tension, even in comparison with the constant viscosity case.

Key words: Dark Matter, Cosmological Parameters

1 INTRODUCTION

New observations on different scales have led us to a more comprehensive understanding of the universe's evolution based on the standard Λ CDM model. However, due to the increasing accuracy of observational data, new issues have emerged on the large cosmic scale, for example, H_0 (the value of Hubble parameter observed today) and σ_8 (the rms fluctuation of density perturbations at $8\ h^{-1}\text{Mpc}$ scale) tensions referring to disagreement between the predicted values of today's expansion rate of the universe and matter clustering from CMB data in comparison with their locally determined quantities (Di Valentino et al. 2021; Schöneberg et al. 2022; Amon et al. 2023).

These issues lead to considering alternative approaches beyond the Λ CDM model such as general relativity modifications or a new description for dark energy (DE) (Huterer & Shafer 2018; da Silva & Silva 2021; Rezazadeh et al. 2022) or different theories of dark matter (DM) (Vattis et al. (2019)). Finding the reason for these apparent discrepancies has become the main driver of cosmological research.

One of the main pillars and components in the standard Λ CDM model is dark matter. The existence of dark matter in our universe is undoubtedly confirmed by numerous kinds of astrophysical observations on a range of length scales from galaxy rotation curves and gravitational lensing to large scale structure (LSS) and the cosmic microwave background (CMB). Nevertheless, the physical nature of DM particles is unclear and an enigma after decades of research, largely because cosmic observations are only sensitive to the gravitational effects of DM rather than the properties of its particles. What we already know about DM in the Λ CDM model is that it is responsible for about 85% of the universe's

matter content and is a non-luminous, dark component of matter which must be largely non-relativistic or cold, massive and collisionless. we consider it as perfect and ideal fluid (Scott 2020; Scolnic et al. 2018).

There are many alternatives to cold dark matter, such as cannibal Dark Matter (Buen-Abad et al. 2018), decaying dark matter (Davari & Khosravi 2022), dynamical dark matter, interacting dark matter (Loeb & Weiner 2011; Archidiacono et al. 2019) and, the interaction between dark energy and dark matter (Davari et al. 2018). In these models, attempts have been made to address some of the tensions of the concordance model resorting to these alternatives.

Among the various models to investigate dark matter from a thermodynamic point of view, an interesting proposal is "an exotic fluid with bulk viscosity". In Anand et al. (2018) is predicted a viscosity of the order of $10^{-6}H_0M_P^2$ by the effective field theory of dark matter fluid on large scales. They claimed that this magnitude of viscosity could resolve the discordance between late time large-scale structural observations and Planck's CMB data.

These viscosities in the cold dark matter can be engendered in two different ways. The first type of viscosity is generated due to the self interaction between the dark matter particles, and they are called "fundamental viscosity". The second type of viscosity is known as "effective viscosity". This kind of viscosity is expected to be generated on large scales as the integrated effect of the back-reaction of small scales non-linearities (Anand et al. 2018).

During the 1940s and 1950s, the first theory to study bulk viscosity was developed, and called Eckart's theory (Eckart 1940). But in the late 1960s and 1970s, it became clear that this type of approach suffered from problems of causality and stability (Muller 1967; Israel & Stewart 1979; D. Pavon

& Casas-Vazquez 1982). Therefore, by including the second-order deviations from equilibrium, it led to the second-order or Müller-Israel-Stewart theory (MISNER 1967; Weinberg 1971; Zimdahl 1996). In addition to introducing a new parameter called relaxation time, the second order theory is a more complicated theory than the first order one. Therefore, the first-order theory has received more attention. We will also develop this work using the Eckart framework.

In this paper, we investigate the dynamics of the universe and linear structure formation using Λ viscous dark matter model. Contrary to Anand et al. (2018), we assume that the viscosity parameter is not constant and depends on the dark matter energy density or Hubble parameter, or both these quantities. We notice that assuming such dependences, the total χ^2 gets reduced. Also except for when the viscosity is function of both the Hubble parameter and dark matter energy density, we can alleviate the σ_8 tension better.

This paper is structured as follows: in section 2, first introduce the theory of this model and derive the main equations governing the evolution at background (subsection 2.1) and perturbation (subsection 2.2) levels for different scenarios. Then we review the key features of the background evolution of the universe. We modify the public Boltzmann solver CLASS¹ (the Cosmic Linear Anisotropy Solving System) (Lesgourgues & Tram 2011) for each type of dissipative mechanisms to the dark matter to calculate the cosmological evolution and CMB anisotropies. In section 3, we perform the Markov chain Monte Carlo (MCMC) scans by MONTEPYTHON-v3² (Audren et al. 2013; Brinckmann & Lesgourgues 2019) with a Metropolis-Hasting algorithm using the Planck 2018 TTTEEE+lowl+lowP+lensing data sets (Aghanim et al. 2020) in combination with other probes such as the Baryon acoustic oscillations, BAO (SDSS DR7, BOSS DR12 (Alam et al. 2017), eBOSS Ly- α combined correlations), the Pantheon SNIa catalog (Scolnic et al. 2018) and the cosmic chronometers (CC) data (Camarena & Marra 2018). We review the basic properties and the cosmological effects of viscous dark matter models for the best value of free parameters in Section 4. According to the results obtained in Section 5, we will discuss cosmic tensions and finally conclude in Section 6.

2 PHENOMENOLOGY OF VISCOUS DARK MATTER MODEL

2.1 Background level

In the beginning, we recall the phenomenology of the viscous dark matter models and investigate the effects of viscosity of DM on the solution of Einstein's equation. In the framework of general relativity, we consider that our flat, homogeneous and isotropic universe including radiation, baryons, the viscous dark matter as non-perfect fluid, and dark energy as cosmological constant (Λ) is described by FLRW metric

$$ds^2 = -dt^2 + a^2(t)(dr^2 + r^2 d\theta^2 + r^2 \sin^2 \theta d\phi^2), \quad (1)$$

where $a(t)$ is the scale factor at the cosmic time t .

We write the energy momentum tensor for non-ideal CDM

fluid in the Landau frame, as

$$T_{\mu\nu} = \tilde{T}_{\mu\nu} + \Delta T_{\mu\nu}, \quad (2)$$

where $\tilde{T}_{\mu\nu}$ is the energy-momentum tensor of a perfect fluid, i.e.

$$\tilde{T}^{\mu\nu} = (\rho + p)u^\mu u^\nu + pg^{\mu\nu}. \quad (3)$$

Here ρ is the energy density and p the pressure in the fluid rest frame and $\Delta T_{\mu\nu}$ in the first order gradient expansion is a tiny perturbation that corresponds to all dissipative processes (heat flux, anisotropic-stress, and bulk viscosity) (Weinberg 1971) as

$$\Delta T_{\mu\nu} = \Pi_B(u^\mu u^\nu + g^{\mu\nu}) + \Pi^{\mu\nu}, \quad (4)$$

where Π_B and $\Pi^{\mu\nu}$ represent bulk stress and shear stress tensor respectively defined as

$$\Pi_B = -\xi u^\gamma_{;\gamma}, \quad (5)$$

$$\Pi^{\mu\nu} = 2\eta\sigma^{\mu\nu} = \quad (6)$$

$$-2\eta \left[\frac{1}{2}(\Delta^{\mu\alpha}\Delta^{\nu\beta} + \Delta^{\mu\beta}\Delta^{\nu\alpha}) - \frac{1}{3}\Delta^{\mu\nu}\Delta^{\alpha\beta} \right] \nabla_\alpha u_\beta,$$

where η and ξ represent shear and bulk viscosity. As shear viscosity is a directional process, the cosmological principle precludes its existence in the FLRW metric. Hence, only bulk viscosity is a unique process that is allowed to occur in an expansive, homogeneous, and isotropic background.

Hence, let us examine the expressions 5 in more detail

$$u^\gamma_{;\gamma} = \frac{1}{\sqrt{-g}}\partial_\gamma(\sqrt{-g}u^\gamma) = \frac{1}{\sqrt{-g}}\partial_\gamma(\sqrt{-g})u^\gamma + \partial_\gamma u^\gamma, \quad (7)$$

where

$$\sqrt{-g} = r^2 \sin^2 \theta a^3(t),$$

and

$$(\partial_\gamma(\sqrt{-g})u^\gamma) = (\partial_0\sqrt{-g})u^0 = 3r^2 \sin^2 \theta a^2(t)\dot{a}(t).$$

So that

$$\frac{1}{\sqrt{-g}}\partial_0(\sqrt{-g}) = 3\frac{\dot{a}(t)}{a(t)} = 3H,$$

means that bulk viscosity modifies the effective pressure as $p_{\text{eff}} = p - 3H\xi$ which consists of a sum of two terms, equilibrium pressure p and bulk viscosity pressure, $-3H\xi$.

Choosing a reference frame in which the hydrodynamics four-velocity u_μ is unitary, we can write Equation 2 for imperfect viscous dark matter fluid as

$$\tilde{T}^{\mu\nu} = (\rho + p_{\text{eff}})u^\mu u^\nu + p_{\text{eff}}g^{\mu\nu}. \quad (8)$$

From the conservation of energy, $\nabla_\mu T^\mu_\nu = 0$, assuming that no interactions take place among the cosmic fluid components the continuity equations take the form,

$$\dot{\rho}_r + 4H\rho_r = 0 \implies \rho_r = \rho_{r0}a^{-4}, \quad (9)$$

$$\dot{\rho}_b + 3H\rho_b = 0 \implies \rho_b = \rho_{b0}a^{-3}, \quad (10)$$

$$\dot{\rho}_{\text{vdm}} + 3H(\rho_{\text{vdm}} - 3H\xi) = 0, \quad (11)$$

$$\dot{\rho}_\Lambda = 0 \implies \rho_\Lambda = \rho_{\Lambda 0}. \quad (12)$$

The dynamics of the Universe containing these components is given by the Friedmann equation:

$$H^2 = \left(\frac{\dot{a}}{a}\right)^2 = \frac{8\pi G}{3}(\rho_r + \rho_b + \rho_{\text{vdm}} + \rho_\Lambda). \quad (13)$$

¹ https://github.com/lesgourg/class_public

² https://github.com/audren/montepython_public

Using the definition of the dimensionless energy density parameter $\Omega_{i,0} = \frac{\rho_{i,0}}{\rho_{\text{cr},0}}$, where $\rho_{\text{cr},0} = 3H_0^2/(8\pi G)$ is the current critical energy density at $a = 1$, the Hubble parameter takes the following form:

$$H^2 = H_0^2 (\Omega_{\text{r}0} a^{-4} + \Omega_{\text{b}0} a^{-3} + y(a) + \Omega_\Lambda), \quad (14)$$

where we define $y(a) = \rho_{\text{vdm}}/\rho_{\text{cr},0}$ and set the present density parameter of radiation (photon+relativistic neutrinos) as $\Omega_{\text{r}0} = \Omega_{\gamma 0}(1+0.2271N_{\text{eff}})$. Here, we put the effective extra relativistic degrees of freedom 3.046 in agreement with the standard model prediction (Aghanim et al. 2020). Applying the Friedman equation, which takes the form of $\Sigma_i \Omega_i = 1$, we can write $\Omega_\Lambda = 1 - \Omega_{\text{r}0} - \Omega_{\text{b}0} + y(1)$. Equation 11 can be rewritten in terms of the scale factor ($d/dt = aH/d a$) and the definition $y(a)$ as follows,

$$a \frac{dy(a)}{da} + 3y(a) - \frac{\tilde{\xi}}{H_0} \sqrt{\Omega_{\text{r}0} a^{-4} + \Omega_{\text{b}0} a^{-3} + y(a) + \Omega_\Lambda} = 0, \quad (15)$$

where we have defined the dimensionless parameter $\tilde{\xi} = 24\pi G\xi$. Equation 15 can be solved numerically by fixing the value $y(a=1) = \Omega_{\text{dm},0}$. However, we implement the continuity equation 11 in `background.c` of the public Boltzmann solver `CLASS` and use the shooting method described in Audren et al. (2014) to compute the present-day dark matter density.

In the rest of the study, we consider four different functional forms of the bulk viscosity coefficient, $\xi(\rho_{\text{vdm}}, H, \rho_{\text{vdm}} H)$:

i- Designated as (M1), we consider ξ as constant. This is the model considered by (Anand et al. 2017).

ii- For the second model (M2), where we assume ξ to be proportional to powers of the energy density of viscous DM, $\xi \left(\frac{\rho_{\text{vdm}}}{\rho_{\text{vdm},0}} \right)^n$ and we would obtain the equation 15 as

$$a \frac{dy(a)}{da} + 3y(a) - \frac{\tilde{\xi}}{H_0} \sqrt{\Omega_{\text{r}0} a^{-4} + \Omega_{\text{b}0} a^{-3} + y(a) + \Omega_\Lambda} \left(\frac{y(a)}{\Omega_{\text{vdm},0}} \right)^n = 0. \quad (16)$$

$$a \frac{dy(a)}{da} + 3y(a) - \frac{\tilde{\xi}}{H_0} \sqrt{\Omega_{\text{r}0} a^{-4} + \Omega_{\text{b}0} a^{-3} + y(a) + \Omega_\Lambda} \left(\frac{y(a)}{\Omega_{\text{vdm},0}} \right)^n = 0. \quad (17)$$

iii- For the third model (M3), we consider ξ to be proportional to powers of the Hubble parameter, $\xi \left(\frac{H}{H_0} \right)^m$ and the equation 15 is given as

$$a \frac{dy(a)}{da} + 3y(a) - \frac{\tilde{\xi}}{H_0} \left(\frac{H}{H_0} \right)^{m+1} = 0. \quad (18)$$

iv- For the fourth model (M4), coefficient is proportional to $\xi \left(\frac{\rho_{\text{vdm}}}{\rho_{\text{vdm},0}} \right)^n \left(\frac{H}{H_0} \right)^m$, and the equation 15 is given as

$$a \frac{dy(a)}{da} + 3y(a) - \frac{\tilde{\xi}}{H_0} \left(\frac{y(a)}{\Omega_{\text{vdm},0}} \right)^n \left(\frac{H}{H_0} \right)^{m+1} = 0. \quad (19)$$

The values assumed for free parameter, ξ in all of the mentioned models are positive for thermodynamical reasons. The standard cold dark matter model is recovered in the limit $\tilde{\xi} \rightarrow 0$ for all models.

2.2 Perturbation Level

In this subsection, we briefly survey the main mathematical form of the linear perturbation theory within the framework of viscous matter dark cosmologies. We consider the density and pressure in terms of spatially homogeneous and isotropic background fields with small spatially varying perturbations: $\rho(x, t) = \bar{\rho}(t) + \delta\rho(x, t)$, $p(x, t) = \bar{p}(t) + \delta p(x, t)$. We assume perturbations in the variables $\delta\rho, \delta p \ll \bar{\rho}, \bar{p}$ up to linear order, and we focus on scalar perturbations only. We use the normalized density contrast $\delta \equiv \delta\rho/\bar{\rho}$ to expand the fluid dynamic equations in dimensionless measures of these perturbations and the velocity divergence $\theta \equiv \vec{\nabla} \cdot \vec{v}$.

Note pressure and its perturbation are not independent quantity and they are related to density as:

$$w = \frac{p}{\rho}, \quad c_s^2 = \frac{\delta p}{\delta \rho}, \quad c_{ad}^2 = \frac{\dot{p}}{\dot{\rho}}, \quad (20)$$

where w , c_s^2 and c_{ad}^2 are the dynamical equation of state, the speed of sound in the medium and the adiabatic sound speed of the viscous DM respectively. Since cold DM is a pressureless ideal fluid, $w = c_s^2 = c_{ad}^2 = 0$. The dynamical equations which govern the evolution of cosmological perturbations in Fourier space can be written in Synchronous gauge as

$$\dot{\delta} = -3\mathcal{H}(c_s^2 - w)\delta - (1+w)(\theta + \frac{\dot{h}}{2}), \quad (21)$$

$$\dot{\theta} = -\mathcal{H}(1 - 3c_{ad}^2)\theta + \frac{c_s^2}{1+w}k^2\delta - k^2\sigma, \quad (22)$$

and in the Conformal Newtonian gauge as

$$\dot{\delta} = -3\mathcal{H}(c_s^2 - w)\delta - (1+w)(\theta - 3\dot{\phi}),$$

$$\dot{\theta} = -\mathcal{H}(1 - 3c_{ad}^2)\theta + \frac{c_s^2}{1+w}k^2\delta - k^2\sigma + k^2\psi. \quad (23)$$

One can then calculate $w = \frac{-3\tilde{\xi}(\rho_{\text{vdm}}, H, \rho_{\text{vdm}} H)H}{\rho}$ and $c_s^2 = \frac{\tilde{\xi}(\rho_{\text{vdm}}, H, \rho_{\text{vdm}} H)\theta}{a\rho\delta}$ (Anand et al. 2017). In Lesgourgues & Tram (2011), it is assumed that c_{ad}^2 is scale-independent and approximately equal to c_s^2 , assumptions that we take to be valid in the current study. For the evolution of shear stress, we have implemented Non-Cold Dark Matter Fluid Approximation (NCDFMA) in `CLASS` as

$$\dot{\sigma} = -3\left[\frac{1}{\tau} + \mathcal{H}\left(\frac{2}{3} - c_{ad}^2\right)\right]\sigma + \frac{4}{3}\frac{c_{\text{vis}}^2}{1+w}(2\theta + \dot{h}). \quad (24)$$

c_{vis}^2 is a new parameter named viscosity speed and in implementation of `CLASS` is assumed as $c_{\text{vis}}^2 = 3wc_{ad}^2$ (Lesgourgues & Tram 2011). We implement the perturbation equations 21- 24 in module `perturbation.c` of Boltzmann code `CLASS`

3 MCMC ANALYSIS

In this section, we present constraints on four viscous dark matter models that we discussed in the previous section. For MCMC analysis we use the Metropolis-Hastings algorithm of the cosmological sampling package `MONTEPYTHON-v3`, connected to an altered version of the Boltzmann Solver `CLASS`. We use the following datasets to perform the statistical inference:

- CMB: One of the most important observables in cosmology due to its well-understood linear physics and sensitivity to cosmological parameters is the CMB. Here, we use Planck 2018 CMB temperature and polarization auto- and cross-correlation, both high- l and low- l and with the full set of nuisance parameters, as well as Planck 2018 CMB lensing in the multipole range $40 \leq l \leq 400$ (Aghanim et al. 2020).

- BAO: Another important data for present and future cosmology is the BAO thanks again to its well-understood linear physics. We use the BAO measurements from the Baryon Oscillation Spectroscopic Survey Data Release 12 (BOSS DR12) (Alam et al. 2017), eBOSS DR14-Ly- α combined correlations (de Sainte Agathe et al. 2019) and, WiggleZ (Kazin et al. 2014).

- SNe Ia: The Pantheon Super Novae (SN) sample consists magnitude measurements for 1048 SNe Ia with redshifts $0.01 < z < 2.3$ (Scolnic et al. 2018). Some recent studies have shown that H_0 tension depends directly on the SN Ia absolute magnitude, M_B (Efstathiou 2021). Therefore here, we consider the M_B as a nuisance parameter in our numerical analysis.

- Cosmic Chronometers (CC): The CC approach is very powerful in detecting the expansion history of the Universe obtained through the measurements of the Hubble parameter. We use the $H(z)$ data points from the most recent, accurate estimates and model-independent data in the redshift range $0.07 \leq z \leq 1.965$ based on the relative age of passively evolving galaxies (the differential-age technique). These data are uncorrelated with the BAO data points (Carmarena & Marra 2018).

We employ the χ^2 statistics to constrain our theoretical model,

$$\chi^2 = \frac{(\mathcal{P}_{\text{obs}} - \mathcal{P}_{\text{th}})^2}{\sigma_{\mathcal{P}}^2}. \quad (25)$$

Above \mathcal{P}_{obs} , \mathcal{P}_{th} and $\sigma_{\mathcal{P}}^2$ indicate the observed value, the predicted value and the standard deviation, respectively. The total likelihood is given by:

$$\chi_{\text{min}}^2 \equiv -2 \ln \mathcal{L} = \chi_{\text{CMB}}^2 + \chi_{\text{BAO}}^2 + \chi_{\text{SNIa}}^2 + \chi_{\text{CC}}^2. \quad (26)$$

Here, in addition to the six free parameters of the standard minimum model, i.e. $(\Omega_b, \Omega_{DM}, 10\theta_{MC}, \ln 10^{10} A_s, n_s, \tau_{\text{reio}})$, the viscous dark matter models introduced in the previous section include at most (ξ, n, m) in the M4 model. Model M1 has one parameter and models M2 and M3 has two parameters. The convergence of chains for each parameter is measured by the Gelman-Rubin criterion and one can obtain acceptable $R-1$ values (i.e. below 0.01 for every parameter) with an iterative strategy (Gelman & Rubin 1992). In Table 1, we report the best and the mean values and 68%CL intervals for main parameters including the total matter density parameter ($\Omega_m = \Omega_B + \Omega_{DM}$), the present-day expansion rate of the Universe or the Hubble constant, H_0 and $S_8 = \sigma_8 \sqrt{\Omega_m/0.3}$ in different scenarios. We also show posterior distributions (1σ and 2σ intervals) as dark and light shaded contours, respectively in Figure 1. Some points in the Figure 1 need to be stressed. First, we can see that the decrease of H_0 values is associated with the increase of Ω_m values and vice versa in both viscous and cold dark matter scenarios but the behavior of $\Omega_m - S_8$ and $H_0 - S_8$ in two scenarios are different. Second, it seems that assuming viscosity improves the S_8 tension for the viscous dark matter

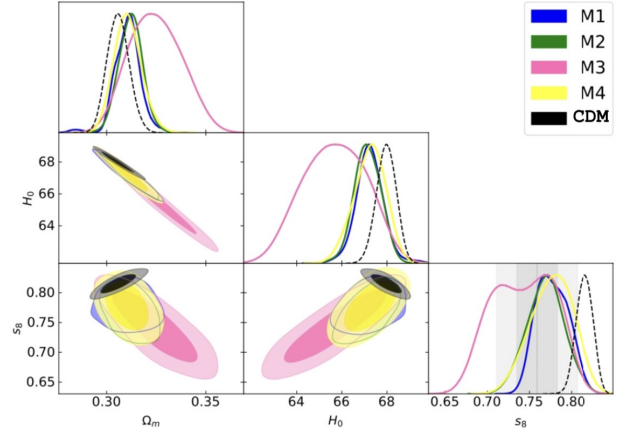


Figure 1. 68% and 95% constraint contours on the matter-density parameter Ω_m , the Hubble parameter, H_0 and S_8 . The grey shaded bands refer to $S_8 = 0.759^{+0.024}_{-0.021}$ from the Kilo-Degree Survey KiDS-1000 (Asgari et al. 2021).

scenario. We will discuss this further in section 5.2.

Next, to check whether the fit is good or not, and also to choose the best and most compatible model with the observational data, we use the simplest method that is usually used in cosmology, which is called the least squares method, χ_{min}^2 . In this case, the model with smaller χ_{min}^2 is taken to be a better fit to the data (Davari & Rahvar 2021). Comparing different viscous models, we note that models M2, M3 and M4 do better than CDM and even M1 scenario where the viscosity parameter was assumed to be constant. The difference between χ_{min}^2 of the M4 model and the CDM model is 4.47. However one should keep in mind that the model with the lowest χ_{min}^2 is not necessarily the best model because since adding more flexibility with extra parameters will normally lead to a lower χ^2 . That means that a poorly parameterized model should be penalized. In this work, M1 model has one parameter, M2 and M3 have two parameters and M4 has three parameters more than CDM scenario. In order to deal with model selection a standard approach is to compute the Akaike Information Criterion (AIC),

$$AIC = \chi_{\text{min}}^2 + 2M + \frac{2M(M+1)}{N-M+1}. \quad (27)$$

Above M is the number of free parameters in the model and N is the number of data points. Therefore in this criterion, we reduce the practical influence of M in χ_{min}^2 in favor of a model with a lower free parameter. Since $N \geq M$ then we neglect the third term in Equation 27. We report the result of MCMC analysis for the best-fit χ^2 per observational data set and compare the viscous DM models to the reference CDM model in Table 2. The results of this analysis can be interpreted with the Jeffreys' scale as follows: there is substantial support for all viscous DM models ($|\Delta AIC| < 2$) and an indication of the consistency of the two scenarios. Among the viscous DM models, the M3 scenario outperforms others.

Table 1. The best values of the free parameters obtained for different considered models by considering different data sets. It is obvious from these values that the H_0 tension is not solved since S_8 tension is unravel.

M1	best-fit	mean $\pm\sigma$
Ω_B	0.04975	$0.04992^{+0.00094}_{-0.00082}$
Ω_{DM}	0.2599	0.2604 ± 0.0060
H_0	67.26	67.25 ± 0.61
S_8	0.7716	0.7688 ± 0.0095
$\xi(10^{-4})$	0.1004	$0.097^{+0.056}_{-0.048}$
M2	best-fit	mean $\pm\sigma$
Ω_B	0.0498	$0.05006^{+0.00085}_{-0.0010}$
Ω_{DM}	0.2609	0.2622 ± 0.0054
H_0	67.36	$67.11^{+0.67}_{-0.59}$
S_8	0.773	0.769 ± 0.022
$\xi(10^{-4})$	0.1294	$0.149^{+0.063}_{-0.074}$
m	-0.1766	$-0.142^{+0.061}_{-0.081}$
M3	best-fit	mean $\pm\sigma$
Ω_B	0.04987	$0.0524^{+0.0021}_{-0.0028}$
Ω_{DM}	0.2623	$0.272^{+0.010}_{-0.012}$
H_0	67.16	$65.71^{+1.5}_{-1.4}$
S_8	0.780	$0.743^{+0.042}_{-0.038}$
$\xi(10^{-4})$	0.09003	$0.20^{+0.13}_{-0.15}$
n	-0.07761	$0.10^{+0.16}_{-0.11}$
M4	best-fit	mean $\pm\sigma$
Ω_B	0.04997	$0.04989^{+0.00096}_{-0.0012}$
Ω_{DM}	0.2621	0.2603 ± 0.0059
H_0	67.14	$67.26^{+0.77}_{-0.63}$
S_8	0.779	$0.777^{+0.028}_{-0.024}$
$\xi(10^{-4})$	0.1011	$0.091^{+0.043}_{-0.079}$
m	-0.02369	$0.04^{+0.13}_{-0.11}$
n	-0.000791	$-0.053^{+0.048}_{-0.054}$
CDM	best-fit	mean $\pm\sigma$
Ω_B	0.04833	0.04867 ± 0.00043
Ω_{DM}	0.2516	0.2571 ± 0.0050
H_0	68.48	67.97 ± 0.42
S_8	0.8201	0.8155 ± 0.0097

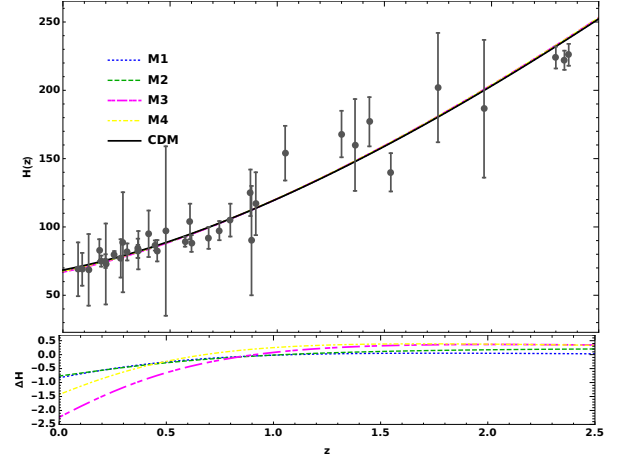


Figure 2. Theoretical predicted the Hubble parameter and their differences as a function of redshift using the best fit values of cosmological parameters in Tables 1 for the proposed viscous dark matter scenarios and CDM model compared to the observational data from cosmic chronometers (Marra & Sapone 2018).

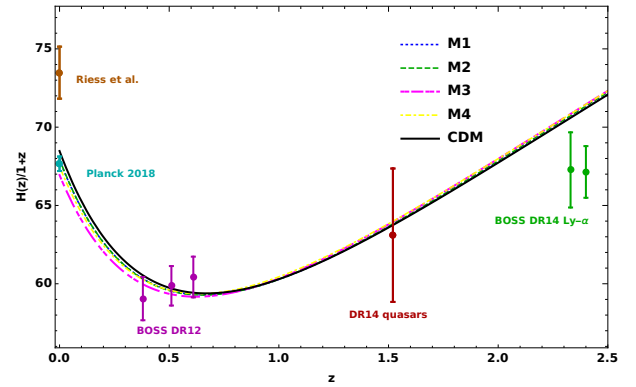


Figure 3. Theoretical comoving Hubble parameter as a function of redshift. Purple triangles show the BAO measurements from BOSS DR12 (Alam et al. 2017), the red circle is from BOSS DR14 quasars (Zarrouk et al. 2018), the green dashed points are the constraint from the BOSS DR14 Ly- α auto-correlation (de Sainte Agathe et al. 2019; Blomqvist et al. 2019).

4 OBSERVATIONAL EFFECTS OF VISCOUS DM MODELS

4.1 Background level

To gain better insight into different models of viscous DM and compare it with the cold DM model, we will examine the evolution of the main cosmological quantities for the parameter values of Table 1 below. As we know one of the key cosmological parameters and a pivotal quantity in cosmology is the current value of the Hubble parameter since it is used to construct the most basic time and distance cosmological scales. On other hand, because of the impact of Hubble's expansion the growth of matter perturbations, it is important to understand the behavior of $H(z)$ in various viscous DM cosmologies. Therefore, we plot the evolution of $H(z)$ and $H(z)/(1+z)$ in Figures 2 and 3. We present in the bottom panel of Figure 2, the relative difference $\Delta H(z) = 100 \times [H_{Mi} - H_{CDM}/H_{CDM}]$ of the Hubble

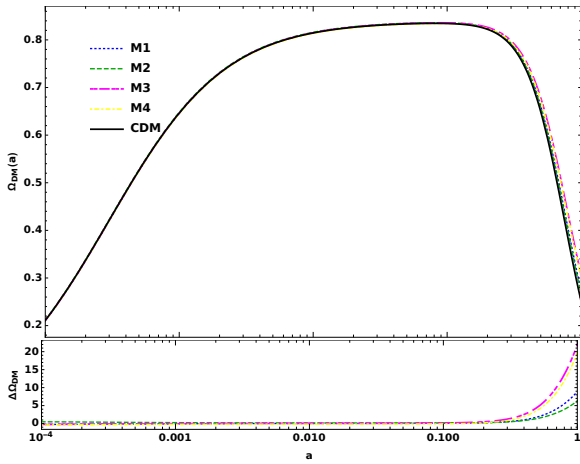
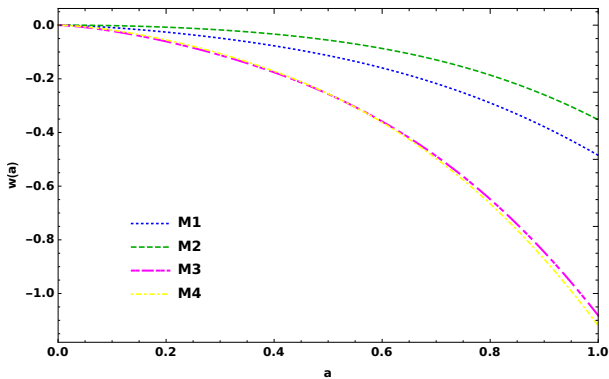
parameters with respect to the CDM. As we see the quantity $\Delta H(z)$ is positive (negative) for large (small) redshifts in all scenarios. But it should be noted that this difference is less for models M3 and M4 and which means that the corresponding cosmic expansion is smaller than that of the concordance CDM.

We have plotted the evolution of the fractional energy densities of viscous dark matter in Figure 4. As we expect all viscous DM models mimic the CDM scenario and the universe evolves from a radiation-dominated phase to a matter-dominated epoch the density parameter of the dark matter decreases and the density parameter of dark energy has increased in the recent universe. Given to reported values in Table 1, the density ratio Ω_{DM}/Ω_B for M3 and M4 models are $\simeq 6$ larger than CDM model ($\simeq 5$).

The last quantity that we plotted in this section is the equation of state parameter for viscous DM, $w = \frac{P}{\rho} =$

Table 2. The result of MCMC analysis for all reviewed models in this study for the best-fit χ^2 per observational data set.

Data Set	M1	M2	M3	M4	CDM
Planckhigh-l-TTTEEE	2359.22	2356.00	2355.14	2356.29	2358.46
Plancklow-l-EE	396.09	395.90	395.69	397.32	396.29
Plancklow-l-TT	22.44	21.81	22.29	22.06	22.72
Planck – lensing	9.10	9.48	9.91	8.38	9.29
Wigglez	817.44	818.53	816.68	817.07	819.07
bao – boss – dr12	5.88	6.05	7.39	6.09	5.91
eboss – dr14 – $ly\alpha$	4.45	4.42	4.50	4.32	4.26
Cosmic – Clock – 2016	14.75	14.73	14.80	14.69	14.70
Pantheon	1026.76	1025.80	1025.72	1025.65	1025.64
χ^2_{\min}	4656.12	4652.72	4652.11	4651.85	4656.32
$-\ln \mathcal{L}_{\min}$	2328.06	2326.36	2326.05	2325.93	2328.16
$ \Delta AIC $	1.8	0.4	0.22	1.53	–

**Figure 4.** The evolution of the fractional energy density of viscous dark matter in terms of scale factor. We use the best fit values from Table 1.**Figure 5.** The evolution of the effective equation of state of viscous dark matter as a function of factor scale.

$\frac{-3\tilde{\xi}(\rho_{\text{vdm}}, H, \rho_{\text{vdm}} H) H}{\rho}$. As we see in Figure 5, in the past (when $a \rightarrow 0$), the viscous DM models behave like CDM ($w \rightarrow 0$), and currently, the value for w is negative for all models. The most negative w are respectively for the M4, M3, M1 and M2 models.

4.2 Perturbation Level

In this subsection, we turn to the perturbation spectra. To draw the plots we have used the best-fit values of the model parameters obtained from all the observational datasets that we have used in this work. First, we display the power spectra of the anisotropies in the CMB temperature, calculated for viscous DM models along with that for CDM in Figure 6. As we can see in the lower multipoles (for $l < 50$), there is a relative deviation of ΔD_l^{TT} between the viscous DM models and CDM scenario. while for higher multipoles (for $l > 50$), we do not observe any significant differences in the curves. We can explain by noting that the CMB temperature is determined only by the energy density component of the energy-momentum tensor, T_{00} , whereas the density perturbations also depend upon the diagonal elements, T_{ii} , which include the pressure. Since the viscous DM scenarios own pressure, this causes a difference between the viscous DM models and CDM. Hence, as the evolution of density perturbations unfolds, small-scale structures are clearly suppressed in viscous DM compared to CDM, which can be seen in the Figure 7. The amount of suppression is larger at smaller k 's. Respectively, models M3, M4, M1 and M2 suppress the nonlinear matter power spectrum.

As we can see in Figures 6 and 8, the position of the acoustic peaks has not shifted therefore the viscous dark matter has not had much effect on the background expansion. We also see a difference between models in the top plane of the Figure 8 for low l . This is due integrated Sachs-Wolfe (ISW) effect at such scales. Also the small l 's of CMB (TT and even better EE) give information on the reionization history. By using the best-fit values of free parameters, shown in Tables 1, we obtain the redshift of the reionization 7.69, 6.99, 8.42 and 8.65, respectively for models M1, M2, M3 and M4. M2 and M4 have the biggest differences with the standard model ($z_{\text{reio,CDM}} = 7.78$).

The present galaxy surveys provide powerful observational data for the combination $f\sigma_8(z)$, where f is the linear growth rate of the density contrast, which is related to the peculiar velocity in the linear theory, being defined by $f(a) = a \frac{\delta'(a)}{\delta(a)}$ and $\sigma_8(a) = \sigma_8(a=1) \frac{\delta(a)}{\delta(a=1)}$ is the root-mean-square mass fluctuation in spheres with the radius $8h^{-1}$ Mpc. Here, we calculate the total density contrast of

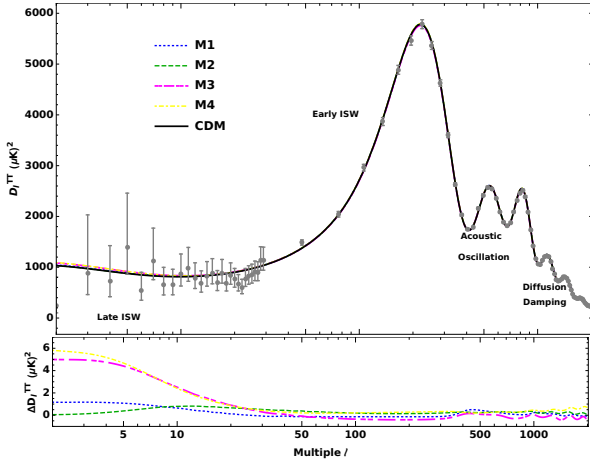


Figure 6. Temperature anisotropies in the CMB calculated for various viscous DM using the best-fit values of various free and derived parameters have been shown in Tables 1. The bottom part of the panel displays the relative temperature differences between the models and CDM model. Physical processes which provide dominant contributions on different scales are quoted (Sugiyama 2014).

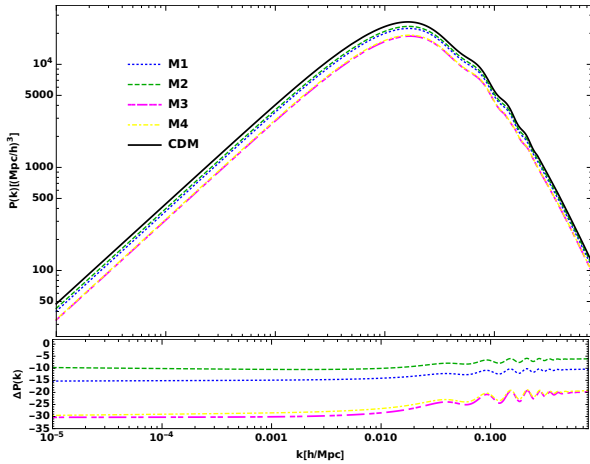


Figure 7. Non-linear matter power spectrum in $z=0$ for various viscous DM and CDM models and the fractional difference between them. As we see for all viscous dark matter cases suppress $P(k)$ The model parameters are the same as in Figure 6.

the matter (baryons + dark matter) as

$$\delta(a) = \frac{\delta_b \rho_b + \delta_{dm} \rho_{dm}}{\rho_b + \rho_{dm}}. \quad (28)$$

The linear growth rate, f , is an excellent tool for distinguishing between various dark matter theories based on the growth of large-scale structures. In Figure 9 we show the linear growth factor $f(a)$ for the different viscous DM and standard models studied in this work for the best-fit values for modes $k = 10^{-4} \text{Mpc}^{-1}$ (the galaxy cluster scale) and $k = 1 \text{Mpc}^{-1}$. Since the linear growth rate is independent of the wave number k at the large scale factors (the low redshift regime), we see that for $a \rightarrow 1$, two modes behave similarly. The bottom panel shows that for small-scale fac-

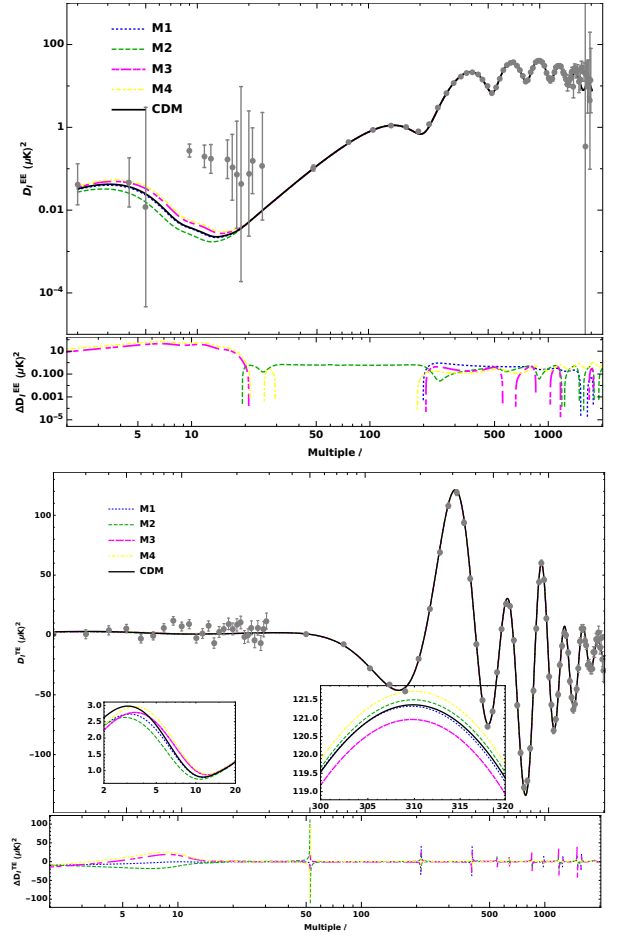


Figure 8. Planck 2018 EE and TE power spectra.

tors the growth function goes to unity, which corresponds to the matter-dominated Universe and the amplitude of matter perturbations decreases at low redshifts in all scenarios with the dominance of dark energy. We observe that the suppression of the amplitude of matter fluctuations in M3 and M4 models that are proportional to the Hubble parameter starts sooner compared with other scenarios. The change in σ_8 in the viscous DM scenarios can be seen as the relative decrease in $P(k)$ in the Figure 7 (although σ_8 is computed from the linear rather than non-linear power spectrum), thus improving the tension between these CMB-derived predictions and the actual LSS data. Looking at Figure 10, we notice that considering viscosity has the influence of slowing down the evolution rate of the dark matter perturbations. This means that structures cluster slower in the viscous dark matter models as we predicted from Figure 7. In particular scenario M4 and M3 suppress the power spectrum more in comparison with the CDM scenario.

5 LARGE-SCALE COSMIC TENSIONS

In this section, we reported the obtained results for the H_0 and S_8 tensions.

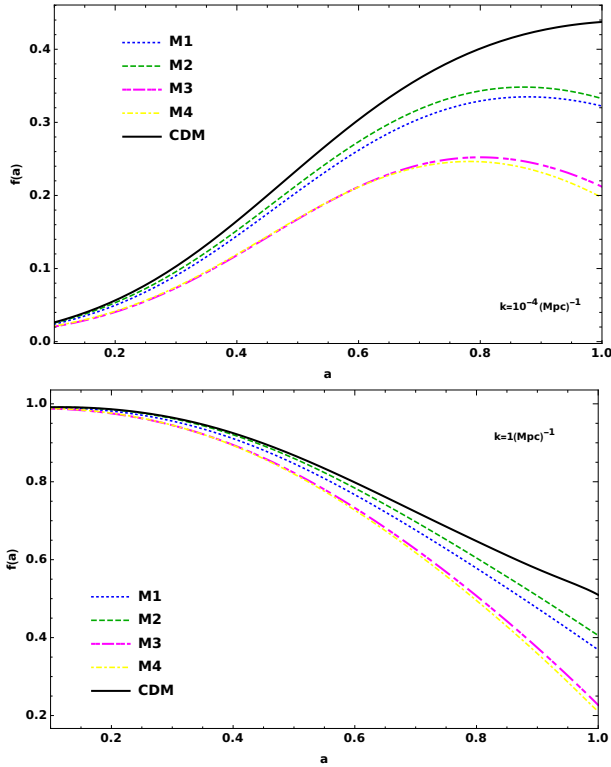


Figure 9. The linear growth rate, f (the scalar perturbations) for mode $k = 10^{-4}$ (the galaxy cluster scale) and 1 Mpc^{-1} (the dwarf galaxy scale).

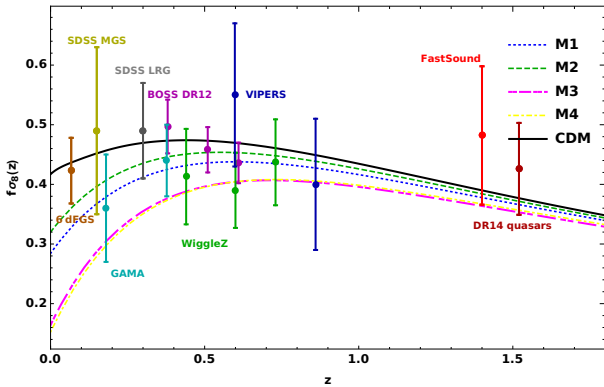


Figure 10. Growth rate of matter fluctuations for our baseline viscous DM models compared to Λ CDM model. The observational constraints are taken from (Aghanim et al. 2020) and references therein.

5.1 H_0 Tension

The Hubble tension is one of the most lingering tensions in the cosmology. This tension emerged with the first release of Planck results and has grown in significance in the past few years. The last value of H_0 tension is obtained from the most recent analysis of Planck 2018 for the early-universe observation $H_0 = 67.44 \pm 0.58 \text{ km s}^{-1} \text{ Mpc}^{-1}$ for the Λ CDM model (Efstathiou & Gratton 2019). While the late-universe observation of Cepheid-calibrated SNe Ia distance ladder by SH0ES team gives the result of $H_0 = 74.03 \pm 1.42$

$\text{km s}^{-1} \text{ Mpc}^{-1}$ (Riess et al. 2019). The big discrepancy between the two H_0 values reaches $\sim 4\sigma$ (Verde et al. 2019; Freedman et al. 2019; Di Valentino et al. 2021). One of the initial motivations of this work was to investigate this tension manipulating the properties of one of the main components of the universe, i.e. dark matter. As the results of Table 1 and Figure 1 demonstrate none of the models of viscous dark matter diminishes the H_0 tension. On the other hand, H_0 tension is equivalent to the mismatch of the Pantheon SNIa absolute magnitudes, which when calibrated using the CMB sound horizon and propagated via BAO measurements to low z have a value $M_B = -19.401 \pm 0.027 \text{ mag}$ (Camarena & Marra 2020b), while when calibrated using the Cepheid stars have a value $M_B = -19.244 \pm 0.037$ (Camarena & Marra 2020a). In this study, for all of the models, absolute magnitudes obtained is ~ -19.41 consistent with CMB observations. Therefore none of these models really help us in addressing the H_0 tension.

5.2 S_8 Tension

Cosmic structures were formed based on primordial density fluctuations that emerged from the inflation era due to gravitational instability. By studying the large-scale structure of the Universe and its evolution in cosmic epochs, it is possible to trace the growth of cosmic perturbations. The main difference between the standard model and other dissipative approaches lies in the behavior of the cosmological perturbations. While perturbations in standard cosmology are always adiabatic, dissipative models of the dark sector are intrinsically non-adiabatic. Associated with this observable, one of the current cosmological tensions is the growth tension. It has come about as the result of the discrepancy between the Planck value of the cosmological parameters Ω_m and σ_8 from weak gravitational lensing surveys, cluster counts, and redshift space distortion data. Since these two parameters have degenerate effects in the lensing surveys, usually $S_8 = \sigma_8 \sqrt{\Omega_m/0.3}$ (Weighted amplitude of matter fluctuations) is used as a parameter to compare the consistency with other observations. Measurements of the CMB temperature and polarization anisotropies by Planck yield $S_8 = 0.834 \pm 0.016$. On the other hand, weak gravitational lensing surveys provide constraints via cosmic shear, e.g. $S_8 = 0.759^{+0.024}_{-0.021}$ from the Kilo-Degree Survey (KiDS-1000) (Asgari et al. 2021) and $S_8 = 0.780^{+0.030}_{-0.033}$ from Hyper Suprime-Cam (HSC) (Hikage et al. 2019). The combination of shear and galaxy clustering from three-year data of DES yields $S_8 = 0.776^{+0.017}_{-0.017}$ and a combination of shear, clustering and galaxy abundance from KiDS-1000 $S_8 = 0.773^{+0.028}_{-0.030}$, while galaxy cluster counts from SPT-SZ report $S_8 = 0.766 \pm 0.025$ and eROSITA results favour $S_8 = 0.791^{+0.028}_{-0.031}$. We adopt the following estimator in order to quantify the discordance or tension in current determinations

$$T_{S_8} = \frac{|S_8^i - S_8|}{\sqrt{\sigma_i^2 + \sigma^2}}. \quad (29)$$

Considering the reported value of the Kilo-Degree Survey KiDS-1000 as observational data, as we see in Table 3, all models of viscous dark matter are able to decrease this tension. More than any of the viscous models, M2 can reduce the tension between Planck and KiDS-1000 data.

Table 3. The result of T_{S_8} for all reviewed models in this study.

Model	M1	M2	M3	M4	CDM
T_{S_8}	0.38σ	0.31σ	0.36σ	0.53σ	2.18σ

6 DISCUSSION AND CONCLUSION

With the aim of finding a model more compatible with the universe and reducing the current controversial tensions in cosmology, this study questioned one of the properties of dark matter in the Standard Model of cosmology. We include a physical dissipation mechanism in the description of dark matter such as viscosity. In addition to the constant bulk viscosity case which was studied previously by Anand et al. (2018), we assessed the cases in which the bulk viscosity has the dependence on ρ_{vdm} , Hubble parameter, or both. We noticed that with such dependences of viscosity, the χ^2 for the cosmological datasets is reduced by roughly ~ 4 . Noting that we have added more parameters we computed the AIC criterion for these models and notice that for all of them $|\Delta AIC| < 2$. The least value for this parameter is obtained for the M3 model, $|\Delta AIC| \simeq 0.22$, where the bulk viscosity is assumed to be proportional to the powers of the Hubble parameter. Our results in Tables 1 and Figure 1 show that the assumption of viscous dark matter can only reduce one of these tensions, namely the S_8 . In order to relax the observed tensions H_0 and S_8 simultaneously, perhaps in addition to viscous dark matter, the presence of relativistic components or early dark energy, should also be considered.

7 ACKNOWLEDGMENTS

This work is supported by Iran Science Elites Federation Grant No M401543.

References

Aghanim N., et al., 2020, *Astron. Astrophys.*, 641, A6
 Alam S., et al., 2017, *Mon. Not. Roy. Astron. Soc.*, 470, 2617
 Amon A., et al., 2023, *Mon. Not. Roy. Astron. Soc.*, 518, 477
 Anand S., Chaubal P., Mazumdar A., Mohanty S., 2017, *JCAP*, 11, 005
 Anand S., Chaubal P., Mazumdar A., Mohanty S., Parashari P., 2018, *JCAP*, 05, 031
 Archidiacono M., Hooper D. C., Murgia R., Bohr S., Lesgourgues J., Viel M., 2019, *JCAP*, 10, 055
 Asgari M., et al., 2021, *Astron. Astrophys.*, 645, A104
 Audren B., Lesgourgues J., Benabed K., Prunet S., 2013, *JCAP*, 02, 001
 Audren B., Lesgourgues J., Mangano G., Serpico P. D., Tram T., 2014, *JCAP*, 12, 028
 Blomqvist M., et al., 2019, *Astron. Astrophys.*, 629, A86
 Brinckmann T., Lesgourgues J., 2019, *Phys. Dark Univ.*, 24, 100260
 Buen-Abad M. A., Emami R., Schmaltz M., 2018, *Phys. Rev. D*, 98, 083517
 Camarena D., Marra V., 2018, *Phys. Rev.*, D98, 023537
 Camarena D., Marra V., 2020a, *Phys. Rev. Res.*, 2, 013028
 Camarena D., Marra V., 2020b, *Mon. Not. Roy. Astron. Soc.*, 495, 2630
 D. Pavon D. J., Casas-Vazquez J., 1982, *Ann. Inst. H. Poincaré*, XXXVI, 79

Davari Z., Khosravi N., 2022, *Mon. Not. Roy. Astron. Soc.*, 516, 4373
 Davari Z., Rahvar S., 2021, *Mon. Not. Roy. Astron. Soc.*, 507, 3387
 Davari Z., Malekjani M., Artymowski M., 2018, *Phys. Rev. D*, 97, 123525
 Di Valentino E., et al., 2021, *Astropart. Phys.*, 131, 102605
 Eckart C., 1940, *Phys. Rev.*, 58, 919
 Efstathiou G., 2021, *Mon. Not. Roy. Astron. Soc.*, 505, 3866
 Efstathiou G., Gratton S., 2019, [10.21105/astro.1910.00483](https://arxiv.org/abs/10.21105/astro.1910.00483)
 Freedman W. L., et al., 2019, ([arXiv:1907.05922](https://arxiv.org/abs/1907.05922))
 Gelman A., Rubin D. B., 1992, *Statist. Sci.*, 7, 457
 Hikage C., et al., 2019, *Publ. Astron. Soc. Jap.*, 71, 43
 Huterer D., Shafer D. L., 2018, *Rept. Prog. Phys.*, 81, 016901
 Israel W., Stewart J. M., 1979, *Annals Phys.*, 118, 341
 Kazin E. A., et al., 2014, *Mon. Not. Roy. Astron. Soc.*, 441, 3524
 Lesgourgues J., Tram T., 2011, *JCAP*, 09, 032
 Loeb A., Weiner N., 2011, *Phys. Rev. Lett.*, 106, 171302
 MISNER C. W., 1967, *Nature*, 214, 40
 Marra V., Sapone D., 2018, *Phys. Rev.*, D97, 083510
 Muller I., 1967, *Z. Phys.*, 198, 329
 Rezazadeh K., Ashoorioon A., Grin D., 2022
 Riess A. G., Casertano S., Yuan W., Macri L. M., Scolnic D., 2019, *Astrophys. J.*, 876, 85
 Schöneberg N., Franco Abellán G., Pérez Sánchez A., Witte S. J., Poulin V., Lesgourgues J., 2022, *Phys. Rept.*, 984, 1
 Scolnic D. M., et al., 2018, *Astrophys. J.*, 859, 101
 Scott D., 2020, *Proc. Int. Sch. Phys. Fermi*, 200, 133
 Sugiyama N., 2014, *PTEP*, 2014, 06B101
 Vattis K., Koushiappas S. M., Loeb A., 2019, *Phys. Rev. D*, 99, 121302
 Verde L., Treu T., Riess A. G., 2019, *Nature Astron.*, 3, 891
 Weinberg S., 1971, *Astrophys. J.*, 168, 175
 Zarrouk P., et al., 2018, *Mon. Not. Roy. Astron. Soc.*, 477, 1639
 Zimdahl W., 1996, *Phys. Rev. D*, 53, 5483
 da Silva W. J. C., Silva R., 2021, *Eur. Phys. J. C*, 81, 403
 de Sainte Agathe V., et al., 2019, *Astron. Astrophys.*, 629, A85